ChemInform Abstract: The Biomedical Chemistry of Technetium and Rhenium

ARTICLE *in* CHEMICAL SOCIETY REVIEWS · MAY 1998

Impact Factor: 33.38 · DOI: 10.1039/A827043Z

The biomedical chemistry of technetium and rhenium

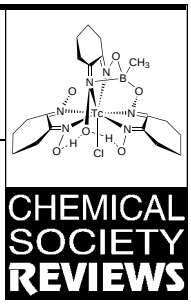

Jonathan R. Dilworth[a] and Suzanne J. Parrott[b]

[a] *Inorganic Chemistry Laboratory, University of Oxford, South Parks Road, Oxford, UK OX1 3QR*
[b] *Department of Biological and Chemical Sciences, University of Essex, Wivenhoe Park, Colchester, UK CO4 3SQ*

This review describes recent developments in the chemistry of both first and second generation 99m-technetium-based imaging agents. The material is presented according to the biological target for the agent, and where possible actual images are presented to indicate the type of information available to the clinician. Beta emitting isotopes of rhenium offer a possible method for the *in situ* treatment of cancerous tissue using analogous targeting strategies to those for technetium. Recent developments in the relevant coordination chemistry of rhenium and their extension to *in vitro* and *in vivo* studies are presented.

1 Introduction

Modern medicine demands progressively more sophisticated methods for the accurate diagnosis of disease states, and there is a massive worldwide research effort into developing and improving imaging techniques. Images can be produced either by measuring the absorption of externally applied radiation (*e.g.* X-ray, ultrasound, MRI imaging), or by administering a small amount of a radioactive compound and detecting the radiation escaping from the body. All of these techniques, enhanced by computerised tomographic methods, can produce remarkably high quality images of locations deep inside the body. To an extent these techniques are complementary, and the method selected will depend not only on the type of image required but also on other factors such as the availability of equipment. Nuclear medicine has traditionally been favoured for imaging biological function, and while some of this area is being taken over by developments in MRI, SPECT (single photon emission computerised tomography) and PET (positron emission tomography) remain the methods of choice for imaging low capacity high density receptors. The use of external radiation for treatment of cancer is extremely well developed, but now the greater ability to target radiopharmaceuticals has led to the possibility of using β-emitting compounds to deliver radiation *in situ* to cancer sites.

In this review we attempt to present a brief account of the major developments in the use of γ-emitting technetium complexes for imaging and recent work directed towards producing β-emitting rhenium compounds for therapeutic use. This is given very much from a chemical perspective, although we have wherever possible given examples of the type of diagnostic image that can be produced. The restriction of space means that it cannot be comprehensive, and the material has been selected to provide what are hopefully interesting illustrations of the potential scope of the radioactive isotopes of Tc and Re for diagnosis or therapy. Technetium-99m, although heavily used (over 90% of all diagnostic nuclear medicine imaging studies carried out worldwide use this isotope) is only one of a range of metallic radionucleides used for medical imaging or therapy, but space restricts our coverage here to Tc and Re. There are several reviews available on Tc and Re chemistry[1–4] and specialised texts[5] and published conference proceedings[6] provide more comprehensive surveys of the medical applications of these elements.

2 Technetium

The element was first predicted by Mendeleev (ekamanganese, number 43) and first isolated by Segré and Perrier in 1938. It was separated from a molybdenum target plate that had been bombarded with deuterons in the Berkeley cyclotron. Currently, there are no fewer than 20 known isotopes (^{91}Tc–^{110}Tc), and seven nuclear isotopes.[7] The ^{99m}Tc nuclear isotope is used for medical imaging due to its near ideal nuclear characteristics of a 6 h halflife and γ-ray emission energy of 141 keV. The diagram in Fig. 1 shows the radioactive decay series involving the medically important Tc isotopes. The practical use of ^{99m}Tc for regular imaging depends totally on the ready availability of

Jon Dilworth graduated from the University of Oxford in 1967 and then studied for a DPhil degree at the Unit of Nitrogen Fixation, University of Sussex, with Professor Joseph Chatt. After a period on the permanent staff of the Unit he took the Chair of Chemistry at the University of Essex in 1985, and has now taken a post in the Inorganic Chemistry Laboratory, University of Oxford (September 1997). His research interests involve the applications of coordination chemistry in biology, medicine and catalysis. Outside he hopes one day to master a top-spin tennis backhand and a reliable method to get out of bunkers.

Jon Dilworth

Suzanne Parrott received a PhD in Chemistry from the University of Essex in 1993 in the area of rhenium coordination chemistry. After working as a Post-doctoral Fellow at The duPont Merck Pharmaceutical Company in Massachusetts, USA she returned to the University of Essex as a Senior Research Officer and is currently a Lecturer in Chemistry at the University. Her research interests include rhenium and technetium coordination chemistry with applications to nuclear medicine.

Suzanne Parrott

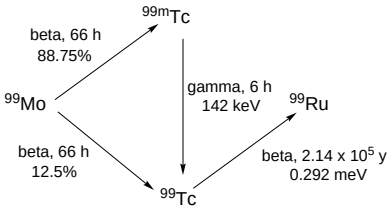

Fig. 1

the isotope using the $^{99}Mo/^{99m}Tc$ generator developed in Brookhaven in the early 1960s. This consists of $[^{99}MoO_4]^-$ absorbed at the top of an alumina ion exchange column. The ^{99}Mo decays continuously to ^{99m}Tc which can be preferentially eluted with physiological saline (0.15 M NaCl) over a period of 7–10 days. A typical eluate used to prepare an imaging agent will be about 10^{-7} to 10^{-8} M in $[TcO_4]^-$. The chemical consequences are that the synthesis of radiopharmaceuticals has to proceed in very dilute aqueous solution directly from $[TcO_4]^-$.

The very dilute nature of the $[^{99m}TcO_4]^-$ solutions means that characterisation of complexes by routine spectroscopic and analytical methods is not possible, and HPLC or other chromatographic methods with γ detection are virtually the only way to monitor the chemistry. The very long lived β-emitting ^{99}Tc isotope is used (typically on a 10–20 mg of technetium scale) to isolate technetium complexes and characterise them fully using the full range of spectroscopic techniques, including X-ray crystallography. HPLC of the ^{99}Tc complexes (UV and β-detection) is then used to infer the structures of the ^{99m}Tc analogues. The weak β-emitting properties of the ^{99}Tc isotope means that complexes can be handled safely in conventional glassware with appropriate precautions. With the widespread use of nuclear reactors, technetium is no longer a rare element and it has been estimated that 160 000 kg of technetium will in principle be available by the year 2000. It is a remarkable statistic that there is already more of this entirely artificial element available in the world than its stable naturally occurring congener rhenium!

Very recently, there have been reports of the preparation of the ^{94}Tc isotope by irradiation of ^{94}Mo in a cyclotron. Both the ^{94m}Tc and ^{94g}Tc isotopes are positron emitters. The ground state isomer also emits γ radiation and offers the interesting possibility of also deploying SPECT. The ^{94m}Tc isotope has been used for PET imaging of the heart using an isocyanide complex (see section 2.3.2 on heart imaging below).

2.1 Imaging techniques for technetium

The eluate from the ^{99m}Tc generator described above is introduced by syringe *via* a septum into a vial containing the reagents necessary to produce the imaging agent. After a suitable incubation period the radiopharmaceutical is injected into the patient, and after time for biodistribution to occur, the image data is collected by a gamma camera equipped with a NaI scintillation detector and photomultiplier system (Fig. 2). The camera is rotated around the patient or a multidetector array is used to create a tomographic image by use of a sophisticated computerised program which reconstruct the image from a series of projections. A successful imaging agent will generally direct in the order of 1–5% of the injected dose of activity to the target organ, the bulk of the remainder generally being excreted *via* the kidneys. The total radiation dose from a technetium scan is comparable with that from a conventional X-ray.

2.2 Types of technetium imaging agents

The first use of technetium for medical imaging was in 1961 and involved the use of $[^{99m}TcO_4]^-$ for diagnosis of thyroid disease, based on the principle that the pertechnetate anion would behave similarly to iodide, known to be taken up by the thyroid. The biodistribution and targeting ability thus depended solely on the size, and charge of the complex. This was the first of a

Fig. 2 A patient undergoing a technetium scan using a gamma camera. Reproduced with permission from Amersham International.

series of the so-called 'technetium essential' or first generation agents. These are represented diagrammatically in Fig. 3(A), and such agents have been deployed with great success to image organs such as the heart, the brain, the kidney and the liver, and are discussed in more detail below. However the growing demand for ever more specific agents has prompted the development of second generation agents [Fig. 3(B)]. Here the targeting capability resides in a biologically active molecule (BAM) covalently linked to an appropriate technetium complex. The BAM is typically a small peptide molecule, which acts as an agonist or antagonist for a specific receptor site, or a monoclonal antibody. The targeting ability of the BAM can be adversely affected by the presence of the technetium complex, and the site of attachment to the BAM, the size, charge and lipophilicity of the conjugate and the length of the covalent linker all need to be optimised for maximum receptor binding.

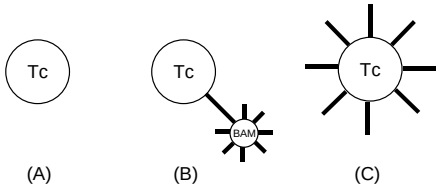

Fig. 3

The ideal situation would be where the outer surfaces of the complex itself contain the groups necessary for receptor binding [Fig. 3(C)]. This approach is far more challenging in terms of the chemistry involved, and developments are currently in the early stages. Examples of all three strategies are presented in the discussions of individual imaging agents below.

2.3 First generation technetium imaging agents

2.3.1 Brain imaging

The dominant requirement for an agent that will accumulate in the brain is that it is capable of traversing the blood–brain barrier (BBB). Viable complexes must therefore be moderately lipophilic and have an overall neutral charge. Research at the University of Missouri in the 1980s demonstrated that a series of neutral amine–oxime complexes could readily be prepared directly from $[TcO_4]^-$ in the presence of $SnCl_2$ as reducing agent. Further development at Amersham International led to the commercially successful Ceretec agent utilising the hexamethylpropyleneamineoxime proligand (HMPAO hexametazime) which loses three protons and forms a neutral, square pyramidal Tc^V mono-oxo complex [Fig. 4(A)].[8] The HMPAO

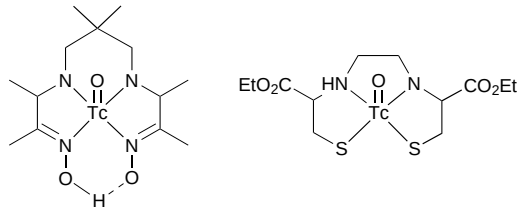

Fig. 4

derivative was selected from more than 100 structural variants for its optimal biodistribution characteristics. The proligand has two chiral centres, and both the D–L and *meso*-HMPAO have been investigated. The greater effectiveness of the D–L complex is dependent on the formation of a more hydrophilic species once the complex has traversed the BBB which prevents diffusion back out of the brain. The mechanism of this reaction is not clear, but glutathione appears to be involved, and the complex from D–L proligand is less stable than that from the *meso*. The Ceretec agent generally has limited stability in solution, and considerable effort has been expanded in increasing the lifetime by addition of agents such as Co^{II}. The Co^{II} is rapidly converted into Co^{III} which is believed to be the active stabilising agent, although the exact details of the mechanism are uncertain. In principle the complex from the *meso* proligand could form two isomeric complexes differing in the orientation of the oxo group relative to the two methyl groups. In practice, only the complex with the Tc=O group *syn* to the methyls has been isolated.

The Tc^V complexes of a wide range of bisamidedithiol proligands have been investigated as potential agents for imaging the brain. The ethylenecysteine diester (ECD) complex is commercially available from Dupont as Neurolite. The proligand loses three protons on reaction with $[TcO_4]^-$ to give the neutral, square pyramidal complex [Fig. 4(B)],[9] which readily crosses the BBB. It provides a striking example of the importance of stereochemistry in determining biochemical function. The L–L form of the complex is trapped once across the BBB due to enzymatic hydrolysis of one ester group by an esterase enzyme, generating a more hydrophilic complex. The corresponding D–D complex is inert to enzymatic hydrolysis and diffuses back across the BBB. Such enzymatic conversion reactions also occur in the blood during biodistribution, and although these impair brain uptake, they facilitate clearance from the blood and non-target tissue *via* the kidneys.

These agents actually provide images of regional cerebral blood flow (rCBF) and these are conventionally presented as computer-generated colour pictures such as that in Fig. 5 obtained using the Ceretec agent. This represents a tomographic slice through a normal brain (front to back, transaxial) with blue–green colours indicating low and orange high Tc concentrations, and therefore high rCBF. The advent of advanced computer techniques has permitted the alternative representation of rCBF as three-dimensional surface rendered images, where blood flow deficits appear as holes in the surface. Fig. 6

Fig. 5 A transaxial scan of a normal brain using Ceretec. Reproduced with permission from Amersham International.

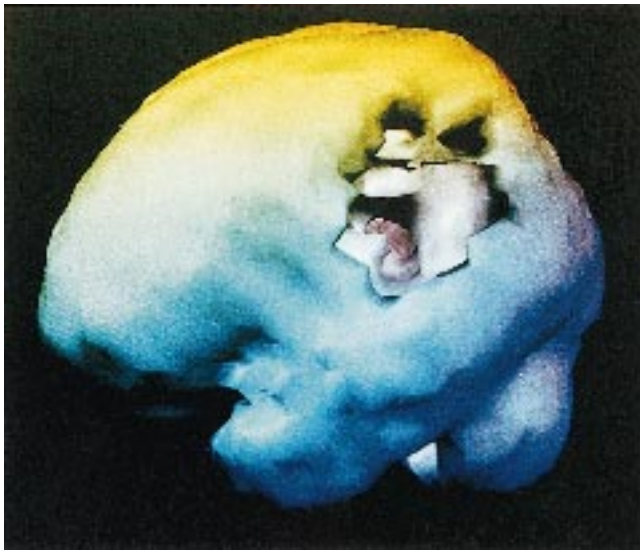

Fig. 6 A three-dimensional surface-rendered SPECT rCBF image for a patient with a stroke in the left upper (parietal) area of the brain. Reproduced with permission from the publishers from M. D. Devous, in *Clinical SPECT Imaging*, ed. E. L. Kramer and J. J. Sanger, ch. 6, Raven Press Ltd, New York, 1995.

provides a dramatic surface rendered ^{99}Tc-SPECT image for a stroke patient with large zone of depleted blood flow in the left parietal area of the brain. The rCBF is dependent on a wide number of factors other than disease, such as anxiety, time of day and cognitive involvement and these have to be taken into account in interpreting the images.

During epileptic fits there is enhanced rCBF (hyper-perfusion) in the site of the EEG abnormality. If EEG is used to monitor the outset of the fit (ictus) then SPECT imaging can be used to image the focus of the abnormality within the brain. The three dimensional surface rendered image in Fig. 7 shows the outline of the area of hyper-perfusion due to the seizure as a

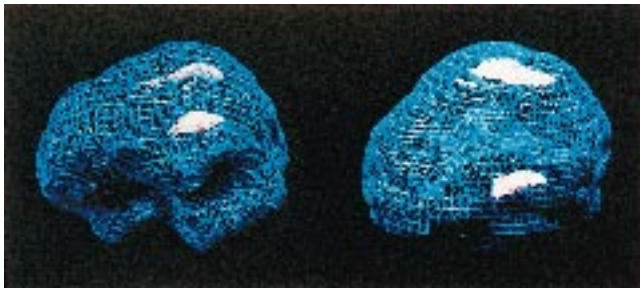

Fig. 7 Three dimensional surface-rendered SPECT images for a patient suffering from seizures. The pinkish area shows the area of hyperfusion during the seizure, and the upper white area indicated secondary activation of the motor region of the brain. Reproduced with permission from the publishers from M. D. Devous, in *Clinical SPECT Imaging*, ed. E. L. Kramer and J. J. Sanger, ch. 6, Raven Press Ltd, New York, 1995.

pink solid body within the brain which is delineated in blue mesh. The white areas in the upper portions of the brain are due to the activation of the sensory motor area that accompanies an epileptic seizure. Such images permit precise location of the site of seizure origin. Subsequent surgical partial temporal lobectomy coupled with drug therapy is the best treatment for seizures which are not responsive to drugs alone.[10] It has been estimated that in the United States alone there are over 50 000 patients suffering from this type of seizure. Only 1% of these are able to have surgical treatment due to the difficulties of locating the focus of the seizure by techniques such as depth EEG.

There are also a number of psychiatric conditions which give rise to characteristic rCBF patterns, and SPECT shows promise to be able to assist in precise diagnosis of such disorders. In schizophrenia there is frequently frontal lobe dysfunction which is particularly evident when the patient is carrying out a task requiring cognitive skills.[11] The left-hand surface-rendered SPECT HMPAO-^{99m}Tc image in Fig. 8 is for a schizophrenic

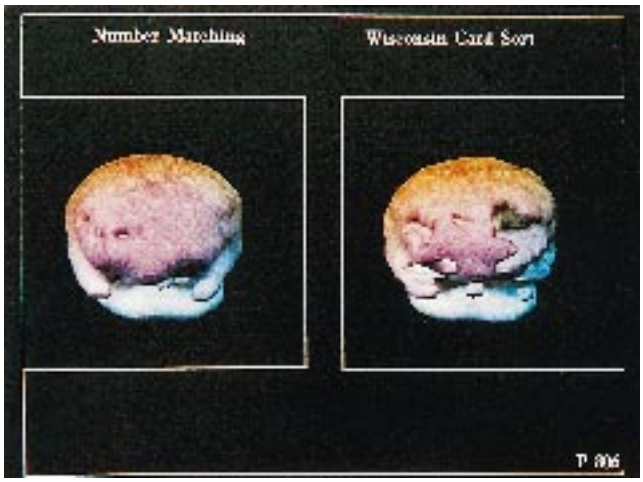

Fig. 8 Three dimensional surface-rendered images for a patient suffering from schizophrenia. The left image was taken while the patient was performing a simple number matching exercise; the right shows rCBF during the Wisconsin card sort exercise which normally would enhance perfusion in the frontal areas of the brain. The decreased flow seen for this patient is typical for schizophrenia. Reproduced with permission from the publishers from M. D. Devous, in *Clinical SPECT Imaging*, ed. E. L. Kramer and J. J. Sanger, ch. 6, Raven Press Ltd, New York, 1995.

patient carrying out a simple task requiring little brain activation. The right-hand image was taken during a Wisconsin Card Sort task which requires intellectual input and would normally result in enhanced perfusion in the frontal lobes. It is characteristic of schizophrenia to observe the decreased perfusion in the frontal lobe of the brain. There have also been reports of altered rCBF patterns in cases of depression, Alzheimer's disease and obsessive-compulsive disorder. The use of ^{99m}Tc labelled neurotransmitter molecules for the possible diagnosis of psychiatric conditions is reviewed below (section 2.4.2).

2.3.2 Heart imaging

Initially it was postulated that lipophilic unipositively charged complexes would accumulate in heart tissue *via* the Na/K ATPase mechanism as K^+ ion mimics. This concept prompted the synthesis of the cationic ^{99m}Tc complex, $[^{99m}Tc(dmpe)_2Cl_2]^+$, where dmpe = 1,2-bis(dimethylphosphino)ethane (Fig. 9) as a potential myocardial perfusion agent.[12]

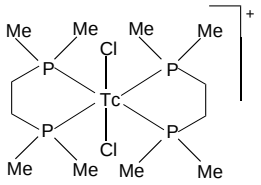

Fig. 9

It was later found that this complex undergoes *in vivo* reduction to the neutral Tc^{II} complex $[^{99m}Tc(dmpe)_2Cl_2]$ which having lost the positive charge has unacceptably fast washout from the heart and accumulates in the liver. Approaches are currently being pursued to lower the susceptibility of the metal ion to reduction which includes evaluation of complexes such as $[^{99m}Tc(diars)_2(SR)_2]^+$, where diars = *o*-phenylenebis(dimethylarsine) and SR^- = thiolate. The thiolate ligands have been shown to increase the reduction potentials of the Tc^{III} complexes relative to the chlorides.

Further development of cationic complexes as myocardial perfusion agents led to the approval and availability of $[^{99m}Tc(MIBI)_6]^+$, where MIBI is 2-methoxy-2-methylpropylisocyanide, Cardiolite which is shown in Fig. 10.[13] The

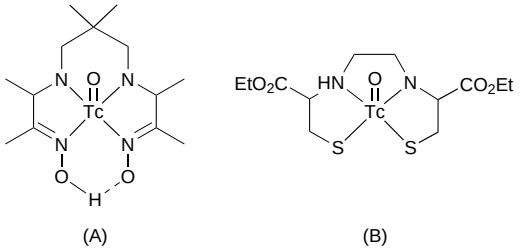

(A) (B)

Fig. 10

X-ray structure of the *tert*-butyl isocyanide ^{99}Tc analogue shows an octahedral arrangement for the isocyanide ligands around the central metal core An investigation into the mechanism of uptake has led to the belief that cations such as $[Tc(MIBI)_6]^+$ accumulate *via* a diffusion mechanism and electrostatic binding due to a high mitochondrial membrane potential. The lipophilicity of the complex is known to be important for uptake into the heart. The Tc^I oxidation state is surprisingly easily accessible directly from pertechnetate as the complex is synthesized by the reaction of $^{99m}TcO_4^-$ with $[Cu(MIBI)_4][BF_4]$ and $SnCl_2$ as reducing agent.

The uptake in the human heart is observed to be about 1.5% of the injected dose which slowly decreases to 1% after 4 h. A good organ to background ratio is achieved due to low uptake in the blood, lungs, liver and spleen. The presence of the alkoxy groups on the monodentate isonitrile ligands is believed to reduce this background activity.

The first approved neutral myocardial perfusion agent is ^{99m}Tc-teboroxime (Cardiotec), Fig. 11, which is a member of the BATO class of complexes, (BATO—boronic acid adducts of technetium dioximes). The complex has the formula $[TcCl(CDO)(CDOH)_2BMe]$, where $CDOH_2$ = cyclohexane-

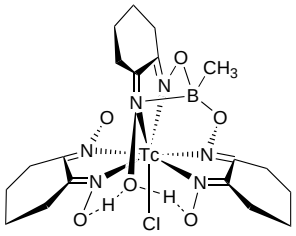

Fig. 11

dione dioxime and is prepared by the reaction of $^{99m}TcO_4^-$ with a mixture of cyclohexane-1,2-dione dioxime and methyl boronic acid with $SnCl_2$ as a reducing agent. 5 Min after injection 2.2% of the injected dose of the Tc^{III} complex is found to accumulate in the heart *via* a mechanism which is unknown at this time, however, the complex exhibits rapid myocardial clearance in normal myocardium.

The complex attains a seven coordinate geometry which consists of the three dioxime ligands bound to the Tc^{III} centre *via* all six nitrogens with one end of the complex capped by a boronic acid derivative. The seventh coordination site is occupied by a chloride ligand.[14] Two protons are believed to be shared between the three uncapped oxime ligands. The chloride ligand has been shown to be labile and susceptible to Cl/OH exchange which may be responsible for the initiation of the mechanism for the fast washout. One mechanism for this washout has been suggested which involves *in vivo* equilibrium between [Tc(OH)(CDO)(CDOH)$_2$BMe] and the cationic complex [Tc(OH$_2$)(CDO)(CDOH)BMe]$^+$. It has been postulated that the neutral complexes may be washed out of the heart and it is the cationic complex which is subsequently retained. This is consistent with the results found with the dmpe complex, [Tc(dmpe)$_2$Cl$_2$]$^+$, previously discussed.

A new class of technetium imaging agents containing the $^{99m}TcN^{2+}$ core, ^{99m}TcN–NOET, has been evaluated for use as myocardial imaging agent. In addition to having a new core it also differs from some other heart imaging agents in not carrying a positive charge, which confirms that the cationic charge for myocardial perfusion imaging agents is not essential. The exact mechanism by which this neutral complex is accumulated in the heart remains to be determined.

An essential feature of the viability of ^{99m}TcN–NOET, where NOET is *N*-ethoxy-*N*-ethyldithiocarbamate, for pharmaceutical use has been the development of a high yield synthesis from methyl-*N*^{2}-methyldithiocarbazate and $^{99m}TcO_4^-$ in the presence of a tertiary phosphine as a reducing agent.[15] This generates a nitride intermediate of uncertain structure in high yield, and subsequent addition of the dithiocarbamate ligand gives the required complex. The lower charge on the Tc≡N^{2+} core as compared with Tc=O^{3+} means that in complexes with comparable ligands the nitrides will generally be more negatively charged. Some recent comparisons of the biological behaviour of oxo and nitrido complexes of DADS and MAG$_3$ (for structures of these ligands see section 2.3.4) support this view. In human volunteers ^{99m}TcN–NOET showed an uptake in the heart of 4.8–5.2% of the injected dose and slow clearance from normal myocardium. The X-ray crystal structure of the analogous dithiocarbamate complex [^{99}TcN(S$_2$CNEt$_2$)$_2$], Fig. 12, shows the technetium to have a five-coordinate square pyramidal geometry with the nitride ligand in an axial site.

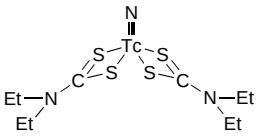

Fig. 12

Two more recent cationic imaging agents which are now in clinical trials are ^{99m}Tc-P53 {a *trans*-dioxobis[bis(2-ethoxyethyl)phosphino]ethane Tc^V cation} also known as tetrofosmine or Myoview, Fig. 13, and ^{99m}Tc-Q12, TechneCard, a mixed N$_2$O$_2$-donor Schiff base/phosphine Tc^{III} cation, Fig. 14. Both complexes carry a single positive charge and contain coordinated phosphine ligands.

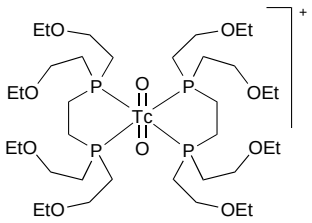

Fig. 13

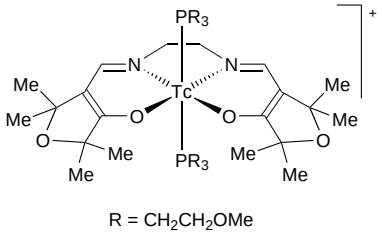

R = CH_2CH_2OMe

Fig. 14

The complex [$^{99m}TcO_2$(P53)$_2$]$^+$, Myoview, is synthesized *via* $SnCl_2$ reduction of $^{99m}TcO_4^-$ in the presence of the diphosphine ligand P53. In contrast to [TcCl$_2$(dmpe)$_2$]$^+$ Myoview contains the dioxo Tc^V core which does not undergo *in vivo* reduction. The complex contains eight alkoxy groups on the bidentate phosphine ligands which help to reduce the background activity in the blood and liver. Uptake of the complex is 1.2% of the injected dose which has slow clearance and reduces to 1% 2 h post injection.[16] Myoview rapidly enters the myocardial cells due to its lipophilic properties and the mechanism of uptake is believed to be similar to that of the ^{99m}Tc-MIBI complex. The dioxobisdiphosphine complex also exhibits rapid lung and liver clearance. The structure of the ^{99}Tc analogue has been determined to be close to octahedral with the two bidentate ligands in the equatorial plane. A representation of the structure is shown in Fig. 13. Fig. 15 and 16 were produced using Myoview, and show a healthy (Fig. 15) and defective heart (Fig. 16). The zone of non-functional heart muscle at the apex of the horseshoe is evident as a dark area. The horseshoe-shaped image is a consequence of the particular cross section of the heart due to the orientation of the scan.

Due to the ease of reduction of [Tc(dmpe)$_2$Cl$_2$]$^+$ ^{99m}Tc-Q12 was designed to incorporate fewer phosphine ligands and so reduce the susceptibility of the metal ion to undergo detrimental reduction. The Tc^{III} complex attains an octahedral geometry with the tetradentate ligand occupying the equatorial plane and the two monodentate tertiary phosphines occupying the axial sites. The Schiff base ligand is 1,2-bis-{[(dihydro-2,2,5,5-tetramethylfuran-3(2*H*)-onato)methylene]amino}ethane which contains a furanone group to aid clearance of the complex from the blood, lung and liver to achieve a good background.[17] Due to the reducing ability of the phosphine ligands the addition of a separate reducing agent such as $SnCl_2 \cdot 2H_2O$ was found not to be necessary.

2.3.3 Liver imaging

Technetium(III) complexes of HIDA [2,6-dimethylphenylcarbamoylmethyl)iminodiacetic acid] derivatives have been shown to be suitable for imaging the hepatobiliary system.[21] Currently there are three ^{99m}Tc-HIDA analogues which have been approved for this purpose; ^{99m}Tc-Lidofenin (TechneScan HIDA) ^{99m}Tc-Mebrofenin (Choletec) and ^{99m}Tc-Disofenin (Hepatolite). The exact nature of the complexes is uncertain but

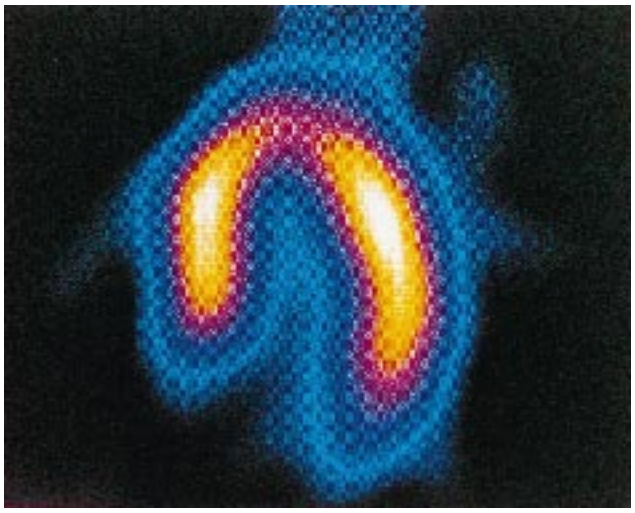

Fig. 15 SPECT image of a normal heart taken using Myoview. Reproduced with permission from Amersham International.

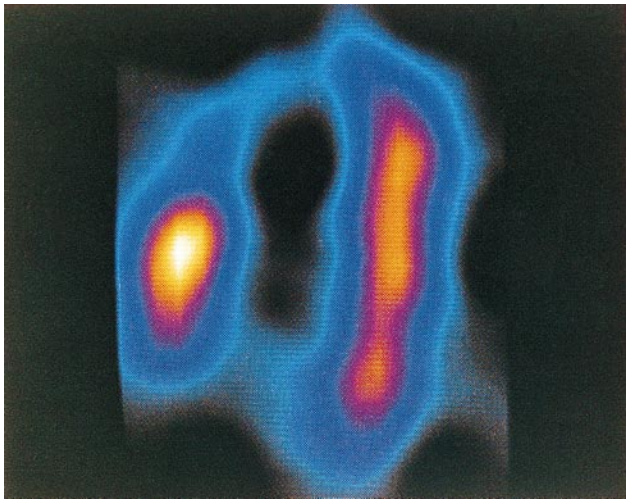

Fig. 16 SPECT image of a diseased heart taken using Myoview. The diseased regions show as gaps in the horseshoe shape seen for the healthy heart. Reproduced with permission from Amersham International.

Fig. 17 shows the proposed structure. The complex is believed to contain two ligands coordinated in an octahedral configuration and bear a single negative charge.

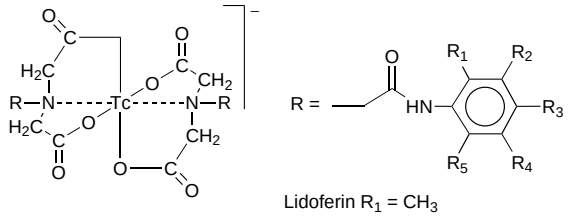

Fig. 17

Tc-sulfur colloid is also used for liver imaging and is believed to be made up of $^{99m}Tc_2S_7$ and colloidal sulfur. The Tc-sulfur colloid is produced by the sodium dithionite reduction of TcO_4^- in an acidic solution. 80–85% of the colloid is accumulated in the liver *via* uptake in Kupffer cells by phagocytosis. A normal liver scan taken using the Tc-colloid is shown in Fig. 18. The two images are taken from the front (upper) and side, and show uptake of the tracer in the liver and spleen (to the right in upper image). Some uptake in the bone marrow of the spine can also be seen (pale purple in the upper image).

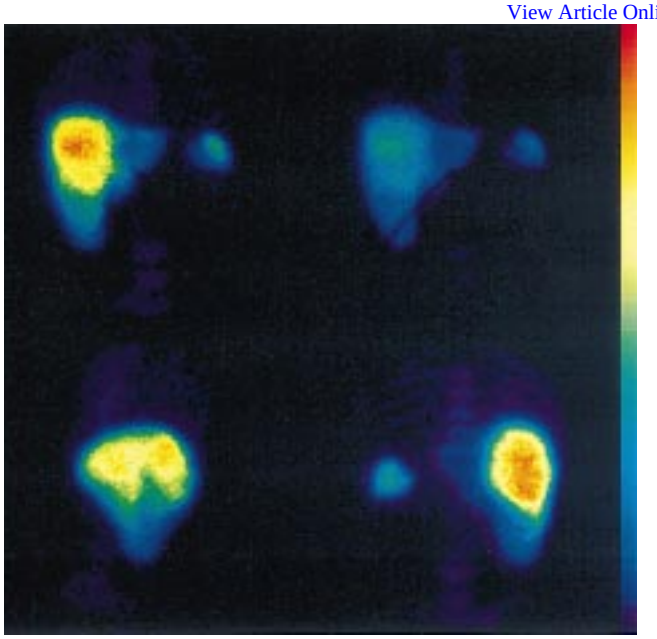

Fig. 18 Liver SPECT images using Tc-sulfur colloid. The upper scan is taken from the front, the lower from the side. The spleen appears as a fainter spot to the right in the upper image, and uptake by the bone marrow is evident with a pale purple outline of the spine. Reproduced with permission from Dr S. J. Mather, Department of Nuclear Medicine, St Bartholomews Hospital, London.

2.3.4 Kidney imaging

$[^{99m}TcO(glucoheptonate)_2]^-$, Glucoscan also known as TechneScan or Glucoheptate, is an early kidney imaging agent, the precise structure of which is unknown, although it is believed to have the five coordinate structure shown in Fig. 19.[18] The

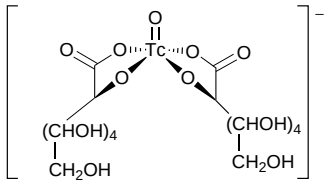

Fig. 19

complex is not currently used widely as an imaging agent due to the availability of better alternatives such as ultrasound and CT X-ray imaging. However, the complex is regularly used as a precursor for the synthesis of other Tc^V species *via* ligand exchange. The complex is synthesized by the reaction of $^{99m}TcO_4^-$ with calcium glucoheptonate in the presence of the reducing agent $SnCl_2 \cdot 2H_2O$.

A ^{99m}Tc-DMSA complex (DMSA is dimercaptosuccinic acid), has been used to image the kidney for a number of years. The Tc^{III} complex (of unknown structure) is prepared from the reaction of $^{99m}TcO_4^-$ with DMSA in the presence of the reducing agent $SnCl_2 \cdot 2H_2O$. Three hours post injection 50% of the injected dose has accumulated in the kidneys and specifically localizes in the proximal convoluted tubule. The Tc^V complex $[TcO(DMSA)_2]^-$ is also known, and the complex has three possible conformations, *syn-endo*, *anti* or *syn-exo*, of the carboxylic acid groups with respect to the Tc=O core. Fig. 20 shows the *syn-endo* orientation. The crystal structure of the analogous rhenium complex $[ReO(DMSA)_2]^-$ has been determined and displays a square pyramidal geometry of the ligands around the central rhenium atom.[20] (see section 3.2.1.2).

^{99m}Tc-DTPA, DTPA = diethylenetriaminepentaacetic acid, has approval for use as a kidney imaging agent. The structure of the ^{99}Tc analogue has not yet been determined and it is unclear at present as to whether the complex contains technetium in the +IV or +V oxidation state. If the complex contains technetium

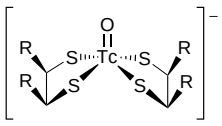

syn endo
R = COOH

Fig. 20

in the +IV oxidation state [Fig. 21(A)] the DPTA is proposed to coordinate as a hexadentate ligand or if the correct oxidation state is +V [Fig. 21(B)] the complex is proposed to contain a pentadentate DPTA ligand and the Tc=O core. In both cases the complex is likely to have octahedral geometry. The complex is prepared by the reaction of $^{99m}TcO_4^-$ with DPTA with $SnCl_2$ acting as a reducing agent.

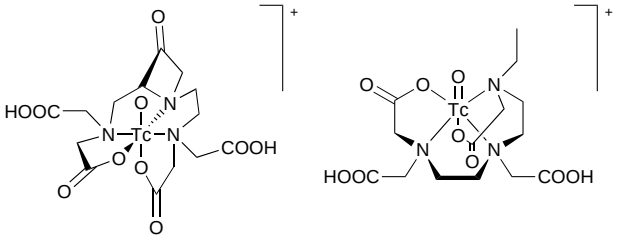

(A) (B)

Fig. 21

Fritzberg[10] developed the most recent and widely used anionic kidney imaging agent, $[^{99m}TcO(MAG_3)]^-$, ^{99m}Tc-O-mercaptoacetyltriglycine, which is shown in Fig. 22.[17] $[^{99m}TcO(MAG_3)]^-$ contains a free carboxylic acid group which is believed to be necessary for efficient renal excretion. The Tc^V

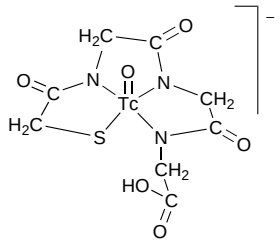

Fig. 22

complex attains a square pyramidal geometry with the oxo group in the apical position. The structure of the rhenium analogue has been determined. In contrast to the previous kidney imaging agents there is no chiral centre and therefore no problems arise from the existence of isomers.The complex is prepared by the reaction of $^{99m}TcO_4^-$ with benzoyl mercaptoacetyltriglycine and the reducing agent $SnCl_2$ when loss of the benzoyl protecting group occurs. The benzoyl protecting group prevents ligand oxidation, and therefore increases kit stability and reliability. A few minutes post injection about 1–2% of the injected dose is found in the kidneys. It is the passage into and through the kidneys which provides a measure of renal function. The presence of the thiol group provides additional reducing power to convert Tc^{VII} to Tc^V and assists in the stabilisation of the complex. Current research is directed at variations in the MAG_3 ligand by substitution of glycine by L-alanine thereby modifying the renal excretion characteristics.

2.3.5 Bone imaging

A series of ^{99m}Tc complexes of phosphonate ligands have been developed as bone-imaging agents. The initial developments in this area used pyrophosphate, but it was later shown that diphosphonates such as methylenediphosphonate [MDP, Fig. 23(A)] gave much improved performance. Typically, the agent is prepared by reaction of the $[^{99m}TcO_4]^-$ generator eluate with MDP in the presence of $SnCl_2{\cdot}2H_2O$ as reductant. The co-ordination chemistry involved is not simple and the number of species formed is dependent on pH, concentration and reductant used. The concentration dependence complicates attempts to characterise the ^{99m}Tc complexes by extrapolation from the ^{99}Tc level, as the concentrations are hugely different (10^{-8} M for ^{99m}Tc, 10^{-3}–10^4 M for ^{99}Tc). There is a consensus that the dominant oxidant state for ^{99m}Tc/MDP is Tc^{IV} and that a mixture of oligomers is formed. At the ^{99}Tc level, reaction of $[^{99}TcBr_6]^{2-}$ with H_4MDP led to the isolation and structural characterisation of a polymeric complex [Fig. 23(B)].[22] A hexameric complex has also been isolated and an X-ray structure determination carried out.

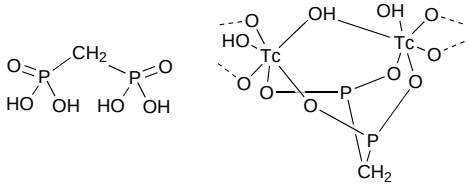

(A) (B)

Fig. 23

The mechanism of absorption on bone is believed to be *via* co-ordination of the free phosphoryl oxygens to calcium ions on the hydroxyapatite bone surface. Since stressed bone has higher concentrations of calcium ions, such areas appear as 'hot spots' on the scan. The ^{99m}Tc-MDP bone scan in Fig. 24 (front and rear view) gives a clear picture of the skeletal structure with an intense (red) area corresponding to the bladder. The area of increased tracer uptake in the right ankle is caused by arthritis.

One of the main uses for ^{99m}Tc bone-scans is for cancer patients to identify if there has been metastasis into the bone, the metasteses appearing as bright spots on the scan. SPECT ^{99m}Tc bone images can in general provide information on lesions which may not be visible by conventional X-ray methods. ^{99m}Tc-based scans can also be valuable for diagnosis of problems with joints such as the elbow or knee, as it can show up bone damage not immediately visible from MRI imaging. Such images then enable the surgeon to screen for those patients who will benefit most from expensive keyhole type exploratory surgery.

2.4 'Second generation' technetium imaging agents

These are classified according to the receptor site or biological function that is targeted.

2.4.1 Steroid receptors

About 60–70% of breast tumours are estrogen receptor positive, and endocrine therapy with drugs such as tamoxifen is effective in about half of cases with such estrogen receptor positive cancers. If a molecule which binds to such sites could be radiolabelled, it would provide a method of monitoring the progress of therapies with agents such as tamoxifen. Most prostate cancers are androgen and progesterone receptor positive and could be imaged with an appropriate labelled receptor hormone. The structures of the three relevant hormones are shown in Fig. 25.

The ^{99m}Tc labelling of the progesterone receptor has been studied utilising conjugation to N_2S_2 ligands *via* a phenyl spacer (Fig. 26).[23] The key to success is to find a site of attachment to the steroid which does not impair receptor binding, and the 11β site proved to be optimal. The conjugates contain stereoisomers, a *syn* pair and two diastereoisomers, and remarkably the *syn* pair had an affinity for the progesterone receptor 161% of progesterone itself. Although the conjugates showed high binding, *in vivo* studies also showed a high level of non-specific binding.

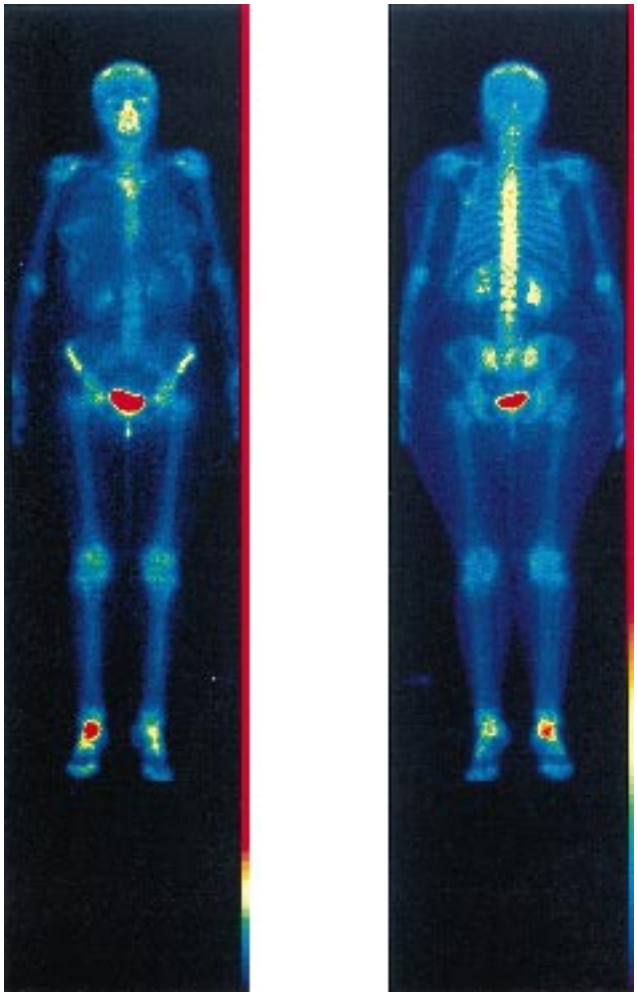

Fig. 24 Bone SPECT images taken using MDP diphosphonate agent. The skeletal structure shows clearly, and the bright red area in the centre is due to accumulation in the bladder. The red area on the right ankle is due to arthritis in the joint. Reproduced with permission from Dr S. J. Mather, Department of Nuclear Medicine, St Bartholomews Hospital, London.

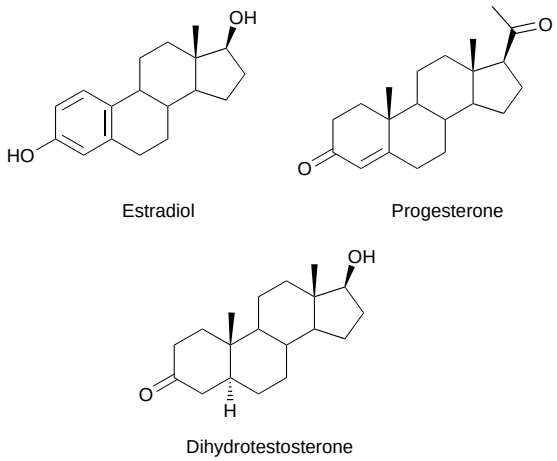

Fig. 25

Nevertheless the approach is clearly promising although further fine-tuning of biodistribution characteristics is required.

An alternative to the pendant receptor ligand approach which was discussed in the introduction above is to integrate the receptor binding sites directly onto the outer periphery of the Tc ligands. A proposed structure for such a complex is shown in Fig. 27(A) and the overall similarity to progesterone is apparent.

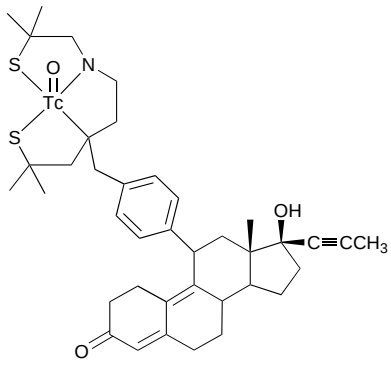

Fig. 26

Some initial steps towards producing an analogue of estradiol (Fig. 25) have been made with the synthesis of the complex shown in Fig. 27(B).[24] Reaction of a Tc^{V} precursor with a 1 : 1 mixture of the two bidentate N–S ligands leads to a good yield of the mixed complex shown rather than a statistical mixture. The receptor-binding affinity was found to be low, as perhaps expected for this initial model, but the approach offers interesting possibilities for the future.

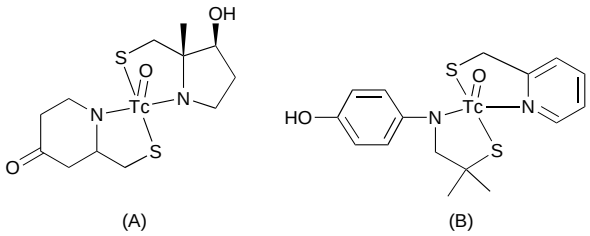

Fig. 27

2.4.2 Central nervous system (CNS) receptors

There are a number of important diseases and psychiatric conditions that are associated with changes in the densities of neurotransmitter receptor sites in the brain: benzodiazepene (epilepsy), muscarinic and nicotinic (Alzheimer's disease), dopaminergic (Parkinson's disease, psychiatric conditions), serotonergic (psychiatric conditions). Most of the initial studies in imaging have used PET, but this imaging modality is of limited availability due to the necessity of being close to a cyclotron. The γ-emitting iodine-123 has been used for SPECT brain receptor imaging, but again this isotope is expensive and unlike ^{99m}Tc, not widely available. There is currently a worldwide effort directed to producing ^{99m}Tc CNS receptor imaging agents *via* the pendant bioconjugate approach. We give two examples of different approaches to the construction of the conjugate.

The molecule ketanserin [Fig. 28(A)] is a potent antagonist for serotonin (5-HT) receptor sites. Detailed biochemical studies have established where modifications can be made without impairing receptor binding and appropriate fragments have been bound *via* thiolate or isocyanide groups to a Tc^{V} oxo-core with a tridentate NS_2^{2-} or SS_2^{2-} ligand.[25] The structure of an Re analogue [Fig. 28(B)] shows the square pyramidal M=O core and the flexible side chain containing the receptor binding sites. Binding studies have been made using rat brain homogenate rich in 5-HT receptor sites and have shown high affinity for the derivative with an OC_6H_5 group in place of the phenyl group and a isocyanide group to provide ligation to the Tc. The higher affinity of this particular derivative appears to be associated with better ability to traverse the BBB.

Cocaine [Fig. 29(A)] and analogues block dopamine transporter sites, and iodine-123 substituted derivatives have been explored for the diagnosis of Parkinson's disease. Linking of the cocaine derivative *via* the seven-membered ring to a Tc^{V} oxo-

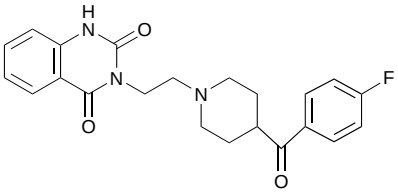

ketanserin

(A)

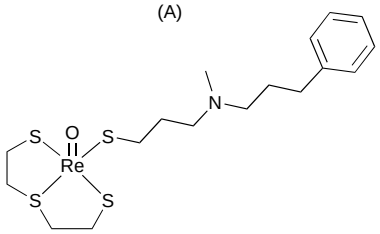

(B)

Fig. 28

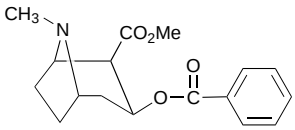

(A)

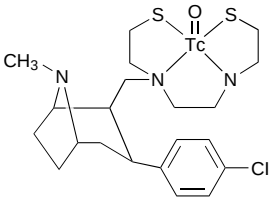

Tc-TRODAT

(B)

Fig. 29

core *via* an N_2S_2 ligand produces a conjugate ('Tc-TRODAT') shown in Fig. 29(B). This has produced the first *in vivo* images of D_2 transporter sites in man (Fig. 30) using technetium-99m. Uptake (coloured yellow) in the areas of the brain rich in D_2

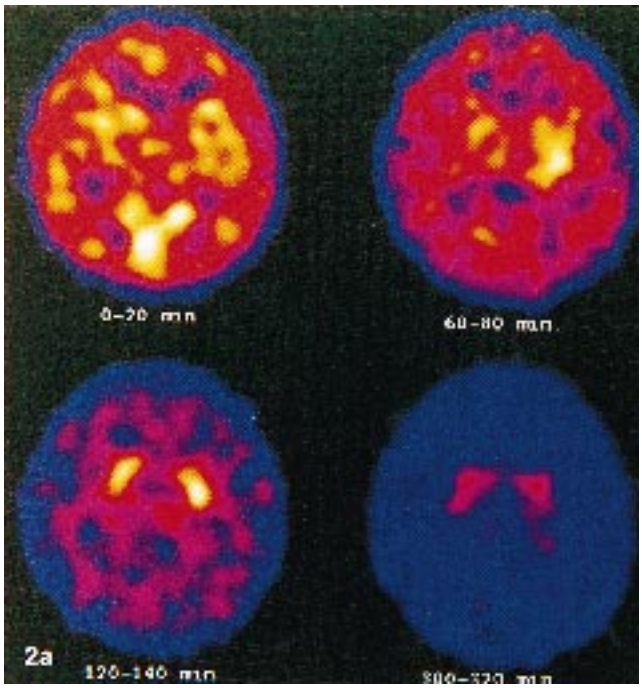

Fig. 30 A series of SPECT scans taken with ^{99m}Tc-TRODAT, at the time intervals shown. The initial image accords with normal rCBF and the 60–80 and 120–140 min scans show significant uptake in the regions of the brain rich in dopamine transporter sites as two bright yellow areas in the centre. Reprinted with permission from H. F. Kung, H.-J Kim, M.-P Kung, S. K. Meegala, K. Plossl and H.-K Lee, *Eur. J. Nucl. Med.*, 1996, **23**, 1527.

receptors is evident in the centre of the image taken after 120 min. This exciting advance confirms the viability of the conjugate approach to the ^{99m}Tc imaging of CNS receptor sites.

2.4.3 Monoclonal antibodies or antibody fragments

Monoclonal antibodies or their fragments, the so-called 'magic bullets', are potentially ideal vehicles to target radioisotopes to specific sites, providing of course the radiolabel can be introduced without interfering with binding to the receptor site. The relatively large size of whole antibodies generally confers undesirably slow biodistribution kinetics for imaging purposes, and attention is now directed to antibody fragments [$F(ab')_2$, Fv, Fab' or Fab] which retain the specific binding characteristics. The use of the fragments also reduces the possibility of immunogenicity and adverse allergic reactions.

The crucial aspect of the development of ^{99m}Tc labelled antibodies and their fragments is the mode of attachment of the metal, and the link must be sufficiently stable to prevent premature release of the radioisotope. The first approach to ^{99m}Tc labelling of antibodies involved the reduction of the disulfide groups holding the $F(ab')_2$ fragments together, and binding of the Tc to the resulting SH groups.[27] Although attractive in its simplicity, the conjugates do not always have high *in vivo* stability. However, Fig. 31 shows a series of images produced by a ^{99m}Tc direct labelled antibody PR1A3 for colorectal tumours. The image after 5 min shows uptake mainly in the heart blood pool and the 7 h image additionally shows liver uptake (below the heart from this angle) and slight uptake in the tumour at 4 o'clock. This tumour uptake has increased significantly after 20 h indicating the relatively slow targeting of the monoclonal antibody.

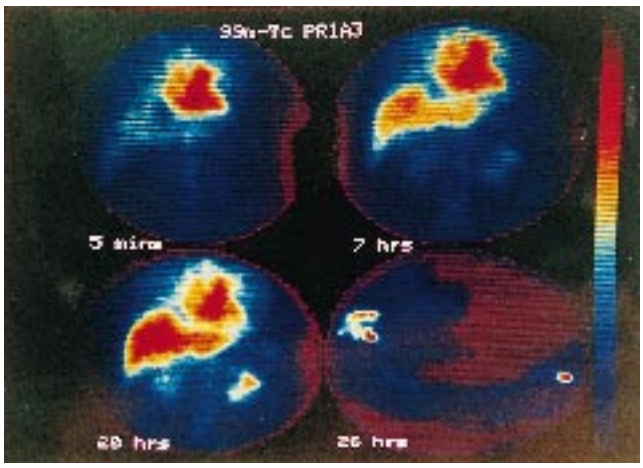

Fig. 31 Scans taken with ^{99m}Tc labelled PR1A3 monoclonal antibody against colorectal tumours at time intervals shown. The 20 h image shows clear uptake in the tumour as a small orange area at 4 o'clock. Reproduced with permission from Dr S. J. Mather, Department of Nuclear Medicine, St Bartholomews Hospital, London.

This has prompted a search for more stable conjugates, and variants of the bifunctional chelate approach appear to offer the most promise. Two principal strategies have been adopted. The first (post-formed chelation) involves initial attachment of metal binding groups to the antibody or fragment followed by insertion of the ^{99m}Tc. Two of the many examples are shown in Fig. 32. A hydrazine nicotinamide derivative can be bound to lysine groups on an antibody or fragment as shown in Fig. 32(A). The hydrazine group then reacts with $[^{99m}TcO_4]^-$ to give an uncharacterised but stable conjugate, which may contain Tc=N–NH– groups. An alternative elegant route to binding the antibody is *via* the thiolactone in Fig. 32(B) which generates an N_2S_2 diaminedithiol ligand system, which forms a stable, neutral, square pyramidal Tc=O species with $[^{99m}TcO_4]^-$.[28]

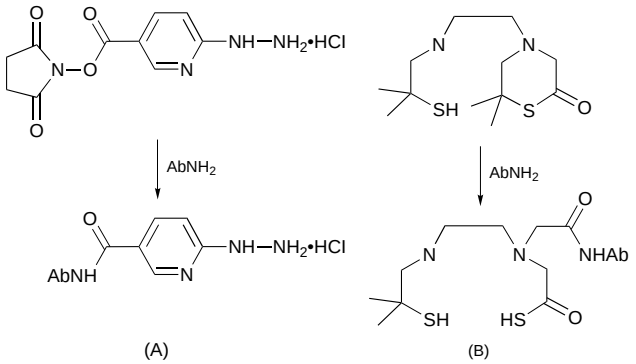

Fig. 32

Antibody engineering techniques have also enabled the incorporation of $(gly)_4$cys peptide into single chain antibody proteins. The peptide binds the ^{99m}Tc in an analogous fashion to mercaptoacetyltriglycine (MAG_3) (see kidney imaging) and provides a stable conjugate. Studies have been made of the protein-coupled fragments of antibodies specific for human ovarian cancer using tumours grafted into mice, and significant uptake of ^{99m}Tc into the tumour was observed.[29]

The alternative approach (preformed chelation) requires the initial synthesis of a technetium chelate with an activated ester group and subsequent attachment of the antibody or fragment. This is illustrated in Fig. 33 for a diamidedithiolate ligand with a pendant tetrafluorophenyl (TFP) activated ester. Kits based on this procedure for attaching antibody fragments for targeting melanoma and lung cancer have undergone chemical trials, and many other related promising systems are currently in development.

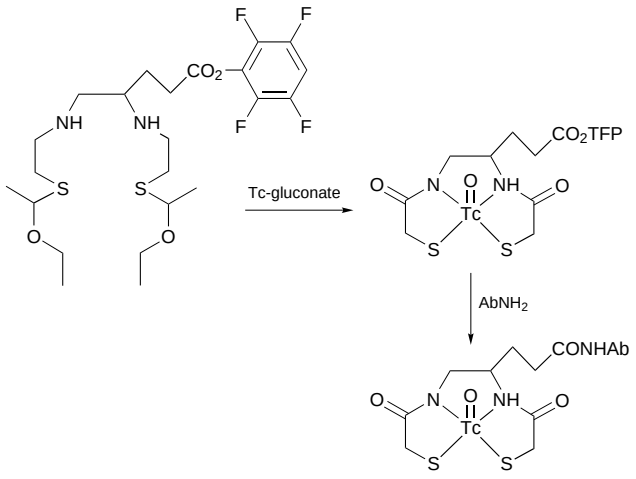

Fig. 33

2.4.4 Imaging hypoxia

Cells become hypoxic in several disease states. A significant fraction of certain types of tumour are hypoxic (80% for head and neck squamous cell carcinoma) and imaging of such tumours would be of great advantage in devising suitable treatments. Impaired blood flow in the heart gives rise to transient or persistent tissue hypoxia, and accurate diagrams of such areas show where medical intervention to restore blood flow would be beneficial. 2-Nitroimidazoles have been shown to be trapped in hypoxic cells due to their reduction to a series of products which either cannot diffuse out or become bound inside the cell.

Several groups have investigated the possibility of linking 2-nitroimidazoles to ^{99m}Tc chelates for hypoxic site imaging.[30] Conjugate A (Fig. 34) shows some promise for hypoxic imaging *in vivo*, but is too lipophilic and clears slowly from background tissue. A more hydrophilic version [Fig. 29(B)] with an oxygen in the backbone is more promising, with more rapid liver clearance.

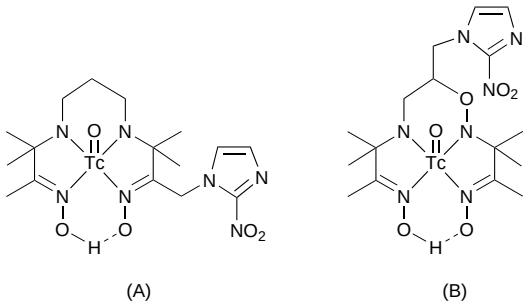

Fig. 34

A variant on this theme involved conjugation of the 2-nitroimidazole to a amineoxime ligand, but with a four- rather than three-carbon backbone (Fig. 35). However, a control experiment for hypoxic imaging using the ^{99m}Tc complex without the imidazole group showed this to be more effective

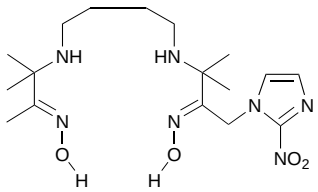

Fig. 35

than with the conjugated imidazole. The co-ordination chemistry of the Tc in this type of amine–oxime complex is strongly dependent on the backbone length. With three carbons in the backbone a monooxo complex is formed, whereas with five carbons a *trans* dioxo system is favoured. The four-carbon system apparently undergoes biochemical reduction and is trapped inside the hypoxic cell. This redox behaviour may be associated with labile protic equilibria involving protonation and/or aquation of the oxo-core. This last complex is showing promise as a hypoxic imaging agent in human clinical trials.

2.4.5 Thrombus imaging

Current research is being directed at the area of diagnostic agents for imaging thrombi. One group has used the approach of conjugating platelet glycoprotein IIb/IIIa antagonists onto a chelate complex of technetium. The glycoprotein IIb/IIIa complex is expressed on the membrane surface of activated platelets and plays an integral role in platelet aggregation and thrombus formation. Cyclic peptides which incorporate the sequence Arg–Gly–Asp (RGD) have been shown to be high affinity antagonists for the glycoprotein receptor.

The glycoprotein IIb/IIIa receptor is expressed only on activated platelets so therefore radiolabelled cyclic IIa/IIIa receptor antagonists were anticipated to bind to only the platelets involved in the thromboembolic event. Fig. 36 shows one example of a technetium complex conjugated to the cyclic glycoprotein IIa/IIIa receptor antagonist. In this case the coordination environment for technetium is based around the N_2S_2 diamide dithiol chelate ligand with the cyclic peptide conjugated onto the backbone *via* an active ester. This complex has also been synthesized from the direct reaction of $^{99m}TcO_4^-$ with the preformed conjugate ligand which eliminates the synthesis of the active ester complex and subsequent step of peptide conjugation.[31] Fig. 37 shows selected images derived from studies of this complex in a dog with implanted deep vein thrombi. The complex was actively incorporated into the growing thrombi with images being clearly detectable within 15 min post-injection.

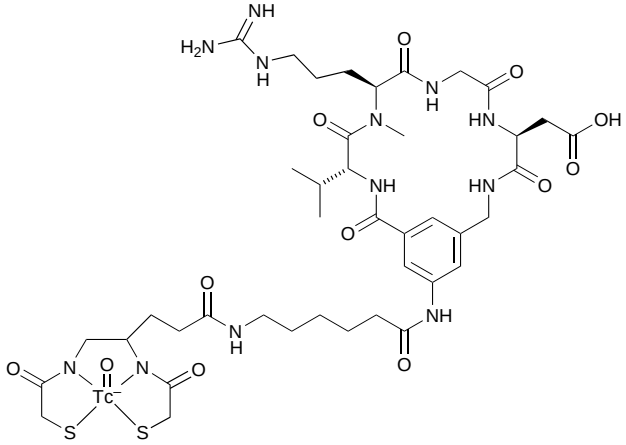

Fig. 36

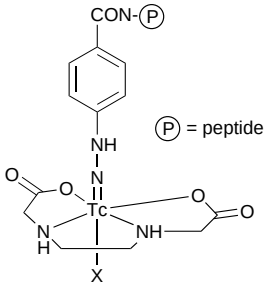

Fig. 38

An alternative mode of incorporation of the cyclic peptide is *via* *N*-hydroxysuccinimidyl hydrazinonicotinate (S-Hynic).[32] Synthesis of the conjugate shown in Fig. 38 was achieved by the reaction of $^{99m}TcO_4^-$ with the Hynic conjugated cyclic peptide in the presence of EDDA (ethylenediaminediacetic acid) and $SnCl_2{\cdot}2H_2O$. The monoanionic ligand X is believed to be chloride, and the hydrazine unit is postulated to be coordinated as an isodiazene ligand (=NNHR) as opposed to a diazenide ligand (–NNR). There is a possibility of a number of isomers for this type of complex. Only investigations at the macroscopic level using technetium-99 or rhenium will confirm the structure of the complex and the mode of coordination of Hynic ligand.

Another group has also investigated the synthesis of technetium complexes containing receptor binding peptides which bind to the glycoprotein IIb/IIIa receptor. They focused on high affinity peptides containing the receptor binding sequence –Apc–Gly–Asp– where Apc is *S*-(3-aminopropyl)cysteine. Again a bisamide bisthiol chelator is used to coordinate technetium which was incorporated into the dimeric peptide. The ^{99m}Tc complex of this peptide P357 was synthesized at room temperature. This complex has given excellent clinical images of deep vein thrombosis and of pulmonary embolism.[33]

3 Rhenium

The element rhenium ($Z = 75$) was discovered in 1925 by the Noddacks and is one of the rarest elements, occurring naturally as a mixture of two non-radioactive isotopes ^{185}Re (37.4%) and ^{187}Re (62.6%). The radioactive isotopes of interest in nuclear medicine are ^{186}Re and ^{188}Re, the nuclear properties of which are summarised in Table 1.

Table 1 Radioactive isotopes of rhenium

	Halflife/ h	Max. β energy/ MeV	Range in tissue/ mm	γ-Energy/ keV
^{186}Re	90	1.07 (71%)	5	137 (9%)
^{188}Re	17	2.1 (100%)	11	155 (15%)

Both isotopes are suitable for therapeutic use by means of β-irradiation. The 5 mm range for ^{186}Re means that it is suitable for small tumours whereas the greater 11 mm range for ^{188}Re is more appropriate for large masses. The selection of isotope is also governed by factors such as halflife and technical aspects of their production. ^{186}Re is generated by neutron radiation of ^{185}Re and there is inevitable contamination with non-radioactive ^{185}Re. On the other hand ^{188}Re is available by radioactive decay of ^{188}W and separable by analogous ion-exchange methods to those used for ^{99m}Tc, and commercial generators are available. Such a generator with 0.5 Ci of ^{188}W has the potential to provide therapeutic treatments to several hundred patients over its 2–6 month lifetime. The major disadvantage of ^{188}Re for therapeutic applications is the relatively short halflife of 17 h.

3.1 Comparison of the chemistry of technetium and rhenium

The 'lanthanide contraction' ensures that the complexes of the two elements are very similar in terms of their physical characteristics (size, lipophilicity, *etc*). Significantly however rhenium complexes are easier to oxidise (harder to reduce) and more kinetically inert than their technetium analogues. The

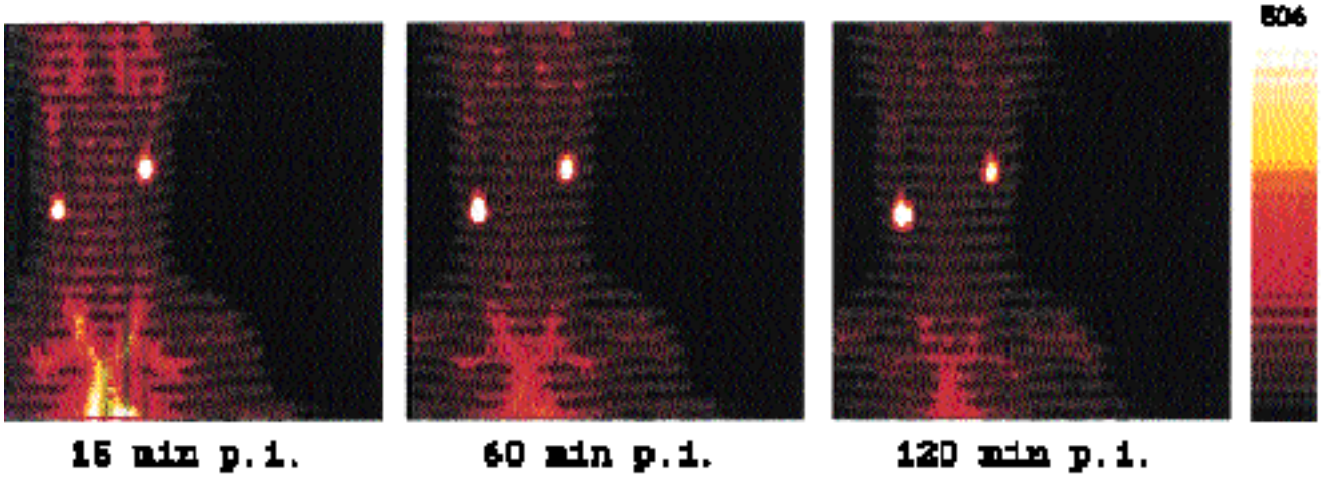

Fig. 37 Images produced by a technetium complex conjugated to a cyclic glycoprotien IIa/IIIa receptor antagonist in a dog with implanted deep vein thrombi. Reprinted with permission from S. Liu, D. S. Edwards, R. J. Looby, M. J. Poirier, M. Rajopadhye, J. P. Bourque and T. R. Carroll, *Bioconj. Chem.*, 1996, **7**, 83. Copyright 1996 American Chemical Society.

relative ease of oxidation of rhenium means that *in vivo* oxidation to $[ReO_4]^-$ is common. This can be an advantage in that it provides an ultimate elimination route for the radioactive isotope *via* the kidneys.

3.2 Rhenium radiopharmaceuticals

3.2.1 'Rhenium essential' agents

As discussed in section 2.2 above this is class of therapeutic agents where the biodistribution is determined by the size, charge and lipophilicity of the complex. Technetium complexes of this type are used to study major organs and there are few examples of rhenium complexes which have the required specificity to be used for treatment of cancers and other therapies.

3.2.1.1 Agents for the palliation of bone pain

Externally applied radiation (sealed source) is widely used for pain relief. However, this is difficult to deploy when metastases are widely distributed through the skeletal structure. This has prompted the search for β-emitting radiopharmaceuticals that can be targeted to bone lesions, and rhenium is one of several radioactive elements under investigation. Among the more developed agents for palliation of bone pain are rhenium radiopharmaceuticals, and are based on diphosphonate ligands.[34] The underpinning co-ordination chemistry is directly analogous to that discussed for ^{99m}Tc bone imaging agents above. Typically $[^{186}ReO_4]^-$ is incubated at 100 °C for 10 min with diphosphonate (HEDP) in the presence of $SnCl_2$ as reductant, giving a 90% labelling yield. As with ^{99m}Tc HPLC measurements indicate that a mixture of polymeric complexes are formed, but bind preferentially to sites of skeletal damage. The exact mechanism by which bone pain is reduced is still unclear, but these agents have proved to be of real benefit in clinical trials.

3.2.1.2 Medullary thyroid carcinoma

A Tc^V complex of dimercaptosuccinic acid (DMSA) is used widely as an agent for the imaging of a relatively rare medullary thyroid carcinoma. The ^{99m}Tc kidney imaging agent using the same ligand is believed to contain Tc^{III} rather than Tc^V. The Re^V complex has the expected square pyramidal structure with an apical oxo-group (Fig. 39), and exists as a mixture of isomers

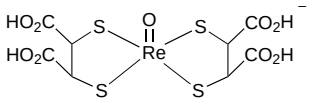

Fig. 39

in solution depending on the orientation of the carboxylate groups with respect to the S_4 plane. This Re complex displays selective uptake in tumour tissue analogous to that of the Tc species, and offers a possibility of therapeutic treatment of this disease.[35]

3.1.2.3 Monoclonal antibodies and fragments

Monoclonal antibodies and their fragments are potentially powerful targeting agents for the therapeutic uses of radionucleides. In principle the methods described in section 2.4.3 above for the attachment of ^{99m}Tc can also be used for the radioactive isotopes of Re. The mercaptoacetyltriglycine (MAG_3) technetium system is used widely as an imaging agent for renal function (see section 2.3.4. above), forming the familiar square pyramidal oxo complex. This system has been adapted by the attachment of an activated ester group *via* an amide group (Fig. 40) to permit conjugation to antibodies or fragments as described above. Conjugation of ^{186}Re to a murine (mouse derived) antibody for adenocarcinomas using this technology gave promising results in animals.[36] The slower kinetics of complex formation for Re means that the preformed

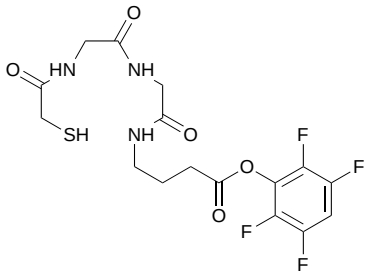

Fig. 40

chelate approach needs to be used as the conditions for complexation of the Re can denature the antibody. Subsequent developments have included using chimaeric human–mouse antibodies which reduced immunogenicity and biodegradable linker groups which accelerate the excretion of non-targeted radioactivity elsewhere in the body as the Re chelate is released and then eliminated by the kidneys.

There have also been studies of the direct labelling of antibodies using the prereduction step to generate free SH groups and subsequent binding to rhenium after stannous chloride reduction of either $[^{186}ReO_4]^-$ or $[^{188}ReO_4]^-$. As with this approach to labelling antibodies with ^{99m}Tc there is a problem with the stability of the conjugates. This is more acute for the therapeutic Re isotopes, as it can lead to undesirable radiation doses at locations other than the tumour.

3.2.1.4 Steroids and bioactive peptides

Certain tumours (pituitary, malignant breast, pancreatic) have a large number of receptors for the tetradecapeptide somatostatin and its cyclic analogue octreotide. The latter has disulfide bridges, and reduction of this and reaction with $^{188}ReO_4^-$/stannous/citrate provides a direct high yield labelling route. Studies in mice have shown that this is retained on injection in tumours and can induce necrosis of the tumour tissue. Bioconjugates of octreotide using the N_2S_2 ligand approach described in Section 2.4 have been made for technetium-99m and have been investigated as a potential method for the imaging of tumours.

Steroids can be attached to rhenium oxo-complexes of N_2S_2 ligand systems in a directly analogous fashion to that described for technetium in Section 2.4.1, and show take up in target tissue rich in steroid receptors. This therefore is a promising approach to the delivery of therapeutic radiation to appropriate tumours. An alternative approach to the labelling of steroids involves the attachment of a rhenium cyclopentadienyltricarbonyl unit to the 17 position of estradiol derivatives as shown in Fig. 41.[37]

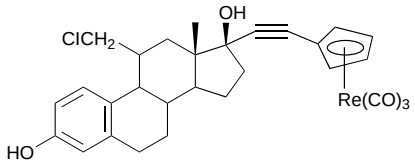

Fig. 41

Surprisingly the derivative (shown) with an 11-chloromethyl group shows higher binding to receptors than the parent steroid. This was attributed to the ability of the acetylene linked Re unit to bend out of the way behind the steroid molecule and an interaction of the CH_2Cl group with a Lewis acid group at the receptor site. It has yet to be shown if this interesting approach can be extended to the radioactive isotopes with the requirement to use aqueous $[ReO_4]^-$ as the starting point for the chemistry.

4 References

Due to the limit on the number of references allowed, the authors have quoted some pieces of work without proper acknowledgement. The choice of work referenced is of necessity somewhat arbitrary, and will we trust not cause offence to those we appear to have ignored.

1 E. Deutsch, K. Libson and S. Jurisson, *Prog. Inorg, Chem.*, 1983, **30**, 75.
2 M. Clarke and L. Podbielski, *Coord. Chem. Rev.*, 1987, **78**, 253.
3 F. Tisato, F. Refosco and G. Bandoli, *Coord. Chem. Rev.*, 1994, **135**, 235.
4 J. R. Dilworth and S. Parrott, *Directions in Radiopharmaceutical Research and Development*, ed. S. Mather, Kluwer, Netherlands, 1996, 1 and other articles therein.
5 *Technetium and Rhenium in Nuclear Medicine*, ed. M. Nicolini, G. Bandoli and U. Mazzi, S. G. Editorali, Padova, 1995, vol. 4 and references therein.
6 *Clinical SPECT Imaging*, ed. E. L. Kramer and J. J. Sanger, Raven Press, New York, 1995.
7 K. Yoshihava, *Top. Curr. Chem.*, 1996, **176**, 2.
8 J. P. Leonard, D. P. Novotnik and R. D. Neirinckx, *J. Nucl. Med.*, 1986, **27**, 1819.
9 E. H. Cheesman, M. A. Blanchette, M. V. Ganey, L. J. Maheu, S. J. Miller and A. D. Watson, *J. Nucl. Med.*, 1986, **29**, 288.
10 B. L. Holman and M. D. Devous, *J. Nucl. Med.*, 1992, **33**, 1888.
11 M. D. Devous, *Brain Imaging, Applications in Psychiatry*, ed. N. Andreason, American Psychiatric Press, Washington, 1988, p. 147 and references therein.
12 M. C. Gerson, E. A. Deutsch, H. Nishyama, K. G. Libson, R. J. Adolph, L. W. Grossman, V. J. Sodd, J. L. Fortman, C. C. Vanderhagden, C. C. Williams and E. L. Salinger, *Eur. J. Nucl. Med.*, 1983, **8**, 371.
13 B. L. Holman, A. G. Jones, J. Lister-James, A. Davison, M. J. Abrams, J. M. Kirschenbaum, S. S. Tubeh and R. J. English, *J. Nucl. Med.*, 1984, **25**, 1350.
14 K. E. Linder, M. F. Malley, J. Z. Gongoutas, S. E. Unger and A. D. Nunn, *Inorg. Chem.*, 1990, **29**, 2428.
15 R. Pasqualini and A. Duatti, *J. Chem. Soc., Chem. Commun.*, 1992, 1354.
16 J. D. Kelly, A. M. Forster, B. Higley, C. M. Archer, F. S. Booker, L. R. Canning, K. W. Chiu, B. Edwards, H. K. Gill, M. McPartlin, K. R. Noyle, I. A. Lathan, R. D. Pickett, A. E. Storey and P. M. Webbon, *J. Nucl. Med.*, 1992, **24**, 353.
17 M. A. DeRosch, J. W. Brodack, G. D. Grummon, M. E. Marmian, D. L. Nosco, K. F. Deutsch and E. A. Deutsch, *J. Nucl. Med.*, 1992, **22**, 850.
18 C. E. Costello, J. W. Brodack, A. G. Jones, A. Davison, D. L. Johnson, S. Kasina and A. R. Fritzberg, *J. Nucl. Med.*, 1983, **24**, 353.
19 J. A. Ponto, H. M. Chilton and N. E. Watson, *Pharmaceuticals in Medical Imaging*, ed. D. P. Swanson, H. M. Chilton and J. H. Thrall, MacMillan Publishing Co., New York, 1990, 501.
20 J. Singh, A. K. Powell, S. E. M. Clarke and P. J. Blower, *J. Chem. Soc., Chem. Commun.*, 1991, 15.
21 A. R. Fritzberg, S. Kasina, D. Eshima and D. L. Johnson, *J. Nucl. Med.*, 1986, **27**, 111.
22 K. Libson, E. A. Deutsch and B. Barnett, *J. Am. Chem. Soc.*, 1980, **102**, 2476.
23 M. J. Welch, J. B. Downer and J. A. Katzenellenbogen, *Current Directions in Radiopharmaceutical Research and Development*, ed. S. J. Mather, Kluwer Academic Press, Netherlands, 1996, p.137 and references therein.
24 D. Y. Chi, J. P. O'Neil, C. J. Anderson, M. J. Welch and J. A. Katzenellenbogen, *J. Med. Chem.*, 1994, **37**, 928.
25 H. Spies, T. Fietz, M. Glacer, H.-J. Pietsch and B. Johanssen, in *Technetium and Rhenium Chemistry and Nuclear Medicine*, ed. M. Nicolini, G. Bandoli and U. Mazzi, S. G. Editorali, Padova, Italy, 1995, vol. 4, p. 243 and references therein.
26 M. E. Kung, H.-J. Kim, M.-P. Kung, S. K. Meegallu, K. Plossl and H.-K. Lee, *Eur. J. Nucl. Med.*, 1996, **23**, 1527.
27 A. R. Fritzberg and D. S. Wilbur, in *Handbook of Targeted Delivery of Imaging Agents*, ed. V. P. Torchilin, CRC Press, Inc., New York, 1995, p. 83 and references therein.
28 D. J. Hnatowich, G. Mardirossan, M. Ruscowski, M. Fargarasi, F. Firzi and P. Winnard, *J. Nucl. Med. Chem.*, 1993, **34**, 172.
29 A. J. T. George, F. Jamar, M.-S. Tai, B. T. Heelan, G. P. Adams, J. E. McCartney, L. L. Houston, L. M. Weiner, H. Opperman, A. M. Peters and J. S. Huston, *Proc. Natl. Acad. Sci.*, 1995, **92**, 8538.
30 C. M. Archer, B. Edwards and N. A. Powell, in *Current Directions in Radiopharmaceutical Research and Development*, ed. S. J. Mather, Kluwer Academic Press, Netherlands, 1996, p. 81 and references therein.
31 S. Liu, D. S. Edwards, R. J. Looby, M. J. Poirier, M. Rajopadhye, J. P. Bourque and T. R. Carroll, *Bioconj. Chem.*, 1996, **7**, 203.
32 S. Liu, D. S. Edwards, R. J. Looby, M. J. Poirier, M. Rajopadhye, J. P. Bourque and T. R. Carroll, *Bioconj. Chem.*, 1996, **7**, 83.
33 J. Lister-James, W. J. McBride, S. Buttram, E. R. Civetello, L. J. Martel, D. A. Pearson, D. M. Wilson and R. T. Dean, in *Technetium and Rhenium in Chemistry and Nuclear Medicine*, ed. M. Nicolini, G. Bandoli and U. Mazzi, S. G. Editorali, Padova, 1994, vol. 3, 269.
34 W. A. Volkert and E. A. Deutsch, in *Advances in Metals in Medicine*, ed. M. J. Abrams and B. A. Murrer, JAI Press, USA, 1993, p. 115 and references therein.
35 P. J. Blower, J. Singh, S. E. M. Clarke, M. M. Bisundan and M. J. Went, *J. Nucl. Med.*, 1990, **31**, 768.
36 A. R. Fritzberg, L. M. Gustavson, M. D. Hylandes and J. M. Reno, in *Chemical and Structural Approaches to Rational Drug Design*, ed. D. B. Weiner and W. B. Williams, CRC Press Inc., Boca Raton, USA, 1994, p. 125 and references therein.
37 S. Top, M. Elhafa, A. Vessieres, J. Quivy, J. Vaissermann, D. W. Hughes, M. J. McGlinchey, J. P. Mornon, E. Thoreau and G. Jaouen, *J. Am. Chem. Soc.*, 1995, **117**, 8372.

Received, 13th June 1997
Accepted, 6th August 1997